

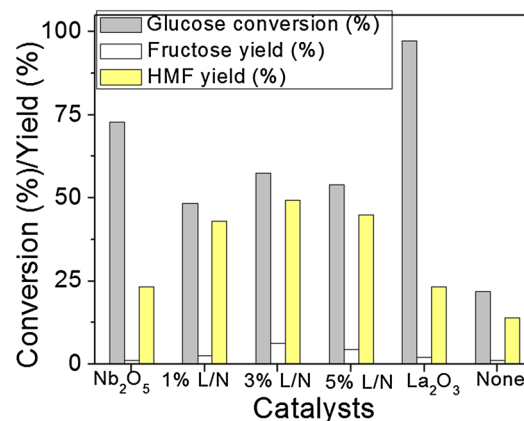
Dehydration of Glucose to 5-Hydroxymethylfurfural Using LaOCl/Nb₂O₅ Catalysts in Hot Compressed Water Conditions

José J. Martínez¹ · David F. Silva¹ · Edna X. Aguilera¹ · Hugo A. Rojas¹ ·
María H. Brijaldo² · Fabio B. Passos² · Gustavo P. Romanelli³

Received: 25 August 2016 / Accepted: 24 April 2017
© Springer Science+Business Media New York 2017

Abstract The dehydration of fructose and glucose to 5-hydroxymethylfurfural was studied using LaOCl/Nb₂O₅ in hot compressed water conditions. The catalysts were prepared by impregnation of LaCl₃ on Nb₂O₅ with different loadings. The solids were characterized by EDX, XRD, TGA and N₂ physisorption at 77 K and pyridine and CO₂ adsorption followed by FTIR; the strength of acidity and basicity was determined by NH₃-TPD and CO₂-TPD, respectively. The use of acid–base systems for HMF production mainly from glucose requires weak basic sites and moderate acidity condition that is reached with LaOCl/Nb₂O₅ as was confirmed by acidity and basicity analyses. The presence of Nb₂O₅ increase HMF yield (>50%) and prevented the formation of undesirable products in hot compressed water conditions, similar results could be obtained with DMSO.

Graphical Abstract



L/N is LaO_x/Nb₂O₅ calcined at 773 K. Reaction conditions: 100 mg of the catalyst and 0.046 M of glucose using using water .

Keywords 5-Hydroxymethylfurfural · LaOCl/Nb₂O₅ · Glucose · Acid–basic solids · Hot compressed water

1 Introduction

The production of 5-hydroxymethylfurfural (HMF) is a current research topic because HMF is expected by the scientific community to become one of the most important chemical building blocks from renewable resources in the near future [1]. 5-Hydroxymethylfurfural can be easily obtained from fructose with high yields in organic or aqueous systems over a diversity of homogeneous and heterogeneous catalysts [2–4]. However, fructose is not abundant in nature and it is expensive [5], which limits HMF large scale production as a sustainable raw material [6]. Therefore, the use of a readily

✉ José J. Martínez
jose.martinez@uptc.edu.co

¹ Escuela de Ciencias Químicas, Facultad de Ciencias, Universidad Pedagógica y Tecnológica de Colombia UPTC, Avenida Central del Norte, Tunja, Boyacá, Colombia

² Departamento de Engenharia Química e de Petróleo, Universidade Federal Fluminense, R. Passos da Pátria, 156, Niterói, RJ 24210-240, Brazil

³ Centro de Investigación y Desarrollo en Ciencias Aplicadas “Dr. J.J. Ronco” (CINDECA), Departamento de Química, Facultad de Ciencias Exactas, UNLP-CCT-CONICET, Calles 47 No 257, B1900 AJK La Plata, Argentina

available and inexpensive sugar such as glucose has been proposed for HMF production [7].

The transformation of glucose to HMF is quite demanding due to glucose–fructose isomerization and fructose dehydration [8]. In particular, niobium oxide (Nb_2O_5) is recognized as a Lewis acid catalyst for the dehydration of glucose to HMF in aqueous phase at 403–443 K showing a high stability [9, 10], and high selectivity to HMF in short reaction times; but substrate conversion was low, between 25 and 50% [9–11].

The use Nb_2O_5 based mixed oxides in this reaction and their properties have not been fully explored. Therefore, there is a need to gain further knowledge on the influence of these systems on HMF production. Recently, tungstite catalysts doped with Nb_2O_5 favored the dehydration of glucose, due of their Lewis and Brønsted acidity balanced; however, this process was favored with the addition of HCl to the reaction mixture [12]. Other example, recently studied was the use of Nb_2O_5 impregnated on $\gamma\text{-Al}_2\text{O}_3$ nanofibers as catalysts for glucose conversion, obtaining a HMF yield of 59% at 423 K at 4 h employing dimethyl sulfoxide (DMSO) as solvent [13]. Lewis acid Nb^{6+} site promoted the isomerization of glucose to fructose, while Brønsted acid sites (originated from Nb–OH–Nb bridge bonds) catalyzed the dehydration of generated fructose to HMF. But, the use of DMSO as solvent has some disadvantages such as low solubility of hexoses, HMF separation problems, and the formation of toxic by-products derived from sulfur decomposition, although DMSO has been the most studied solvent due to highest HMF yields (80%) [14]. Indeed, it is convenient to use water as solvent.

It is well established that in conditions of hot compressed water, the acid–base bi-functionality of oxides used as catalysts promotes a higher HMF yield [15]. We proposed that the use of $\text{LaOCl}/\text{Nb}_2\text{O}_5$ mixed oxides, which contain both acid and basic surface sites, could cause an improvement on HMF yield in hot compressed water conditions. Although the dehydration step could be stimulated by non-catalytic processes (conditions of hot compressed water), and Brønsted acid sites could be generated upon hydrothermal treatment of Nb_2O_5 . In fact, Prado et al. [16] reported that Nb_2O_5 synthesized by a hydrothermal treatment showed an increase in BET area and acidity which influenced the dehydration of glucose. In fact, a synergic effect between the hot compressed water and the acid–base bi-functionality of $\text{LaOCl}/\text{Nb}_2\text{O}_5$ should result in an increase in HMF yield from glucose.

2 Experimental Section

2.1 Materials

Glucose (Panreac, 99%), fructose (Sigma-Aldrich, 99%), 5-hydroxymethylfurfural (Sigma-Aldrich, 99%),

lanthanum(III) chloride heptahydrate (Merck KGaA, 99%), lanthanum(III) oxide (Merck KGaA, 99%), niobium(V) oxide (Merck KGaA, 99%), and methanol (Panreac, 99%) were used without previous purification.

2.2 Catalyst Preparation

Nb_2O_5 was impregnated with $\text{LaCl}_3 \cdot 7\text{H}_2\text{O}$, dried at 373 K and calcined in air at 773 K for 6 h. Calcination of LaCl_3 causes the formation of LaOCl from 773 K [17]. The mixed oxides $\text{LaOCl}/\text{Nb}_2\text{O}_5$ were labelled as LaOCl/Nb .

2.3 Characterization of Catalysts

The elemental analysis of catalysts was carried out by energy dispersive X-ray spectroscopy (EDX). The measurements were performed under vacuum using a Shimadzu EDX-720 spectrometer, with Rh X-ray tube. The powder samples were put in a polyethylene sample cell and covered with a polypropylene film.

The X-ray diffraction measurements were carried out with a Rigaku Miniflex II using $\text{Cu K}\alpha$ radiation ($\lambda = 1.54056 \text{ \AA}$). The XRD patterns were recorded in the 2θ range of 10° – 80° , using a count time of 1 s and a step size of 0.05° . Textural properties of the solids were obtained by N_2 adsorption–desorption isotherms measured at 77 K using a Micromeritics ASAP 2020 equipment. Samples were previously evacuated at 623 K for 12 h. The BET method was used to calculate the total surface area of the samples.

The nature of acid sites was studied by pyridine (Py) adsorption followed by FTIR and temperature programmed desorption of NH_3 . Infrared spectra were collected using a Nicolet iS50 equipment with an in situ diffuse reflectance cell (Harrick, Praying Mantis). For the determination of acid sites, a pretreatment at 673 K was performed with a helium flow of 15 mL/min for 1 h to clean the surface of possible contaminants. Subsequently, the samples were gradually cooled down to 423 K and then pyridine adsorption was performed for 1 h. After adsorption, the gas phase was removed by evacuation with a helium flow (20 mL/min) at 673 K. NH_3 -TPD analyses were performed in a Micromeritics AutoChem II 2920. Prior to the adsorption of NH_3 , the samples were preheated at 673 K in He flow (25 mL/min) for 1 h. Then, adsorption was performed by submitting the sample to 10% NH_3 in helium (50 mL/min) at 393 K for 30 min. The samples were purged with helium (25 mL/min) for 1 h to remove excess of physisorbed ammonia. The TPD began at 393 K with a heating rate of 10 K/min to reach 1173 K. The nature of basic sites was studied by CO_2 adsorption followed by FTIR and temperature programmed desorption of CO_2 . The procedures

were similar to that described for Py-FTIR and NH₃-TPD, only the gas of adsorption was changed to CO₂.

Thermogravimetric analysis was performed using a Setaram thermobalance. 3% LaOCl/Nb₂O₅ powder (60.0 mg) was transferred to an alumina crucible and heated using a 5 K/min heating rate up to 1073 K, under an atmosphere of N₂ flowing at 20 cm³/min.

The solids were submitted to a hydrothermal treatment at 453 K during 2 h, dried at 323 K previously to Raman spectra acquisition. Raman spectroscopy experiments were carried out at room temperature using a Confocal Raman Microscope (Witec, alpha 300) with a 50× objective lens, a Nd:YAG green laser with 532 nm wavelength and 800 scans. Spectra for each solid were taken over the range of 20 and 3000 cm⁻¹, scanning at a step size of 1.0 cm⁻¹ with an integration time constant of 10 s.

2.4 Catalytic Studies

The catalytic activity of the mixed oxide was evaluated in the conversion of fructose and glucose to HMF in a 100 mL stainless steel reactor. The details of reactor can be found in the Ref. [18]. All experiments were conducted in a home-made 300 cm³ STR made of stainless steel 304 SS. In the interior is inserted a Teflon vessel, with a 1 mm thick wall, which guarantees inertia against the reactions.

The reactor was charged with reactants, then sealed, purged with N₂ and pressurized with N₂ to 0.6 MPa. The reactor was heated to desired temperature with a heating jacket and mixing was accomplished with a magnetic stirrer. The initial conditions of reaction were 100 mg of the catalyst, a solution of glucose (0.046 M) in a ratio catalyst/substrate 1:5 using 60 mL of water as solvent. The temperature effect was studied from 333 to 473 K. DMSO was also studied as a reaction solvent because it is the one that has been most reported in the literature.

After 3 h, the reactor was quenched in ice water and the reaction mixture was centrifuged and the recovered solid was weighed. The liquid phase was filtered and analyzed by HPLC in an equipment HP-1100 equipped with a Knauer Eurokat Pb column (300 × 4 mm, 10 μm) using a refractive index detector (for glucose and fructose) and UV detector at 280 nm for quantify HMF. The column temperature was maintained at 353 K and, the mobile phase was water with a flow rate of 0.1 mL/min. The conversion of reactant, product selectivity and product yield were defined as follows:

$$\text{Conv. (\%)} = \frac{\text{initial concentration of glucose} - \text{final concentration of glucose}}{\text{initial concentration of glucose}} \times 100$$

$$\text{Yield of product } y \text{ (\%)} = \frac{\text{concentration of } y \text{ produced}}{\text{initial concentration of glucose}} \times 100$$

$$\text{Selectivity (\%)} = \frac{\text{yield of product } y}{\text{conversion of glucose}}$$

In this study was determined the concentrations of fructose and HMF using the response factors obtained by the IR and UV detector, respectively. Other products were not identified.

3 Results and Discussion

3.1 Characterization of Catalysts

The LaOCl loadings determined by EDX showed values that were similar to nominal expected values (Table 1). The presence of chlorine (Cl) on LaOCl/Nb₂O₅ catalysts could not be detected by EDX analysis, because in the case of chlorine (Cl), a characteristic X-ray from the X-ray tube interferes and overlaps with a target peak (Rh). The energy of the line Kα of Cl is about 2622 keV and that of the line Lα1 is 2697 keV, therefore they are very close.

The surface areas of Nb₂O₅, LaOCl/Nb₂O₅ (LaOCl/Nb) and La₂O₃ are similar, as can be observed in Table 1, in the same manner that the other textural properties (pore size and pore volume). Thus, this values suggests these materials are not porous, so that the pores are arising from interparticle voids.

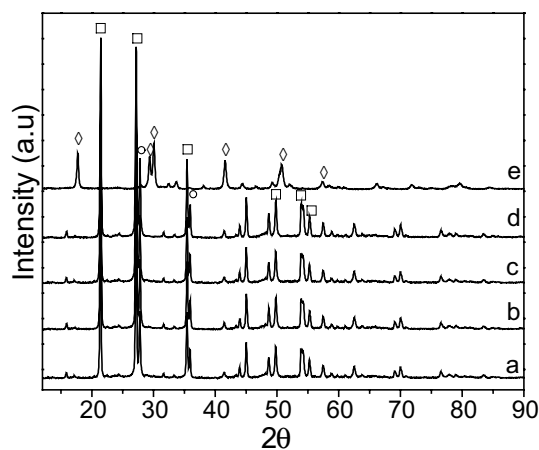
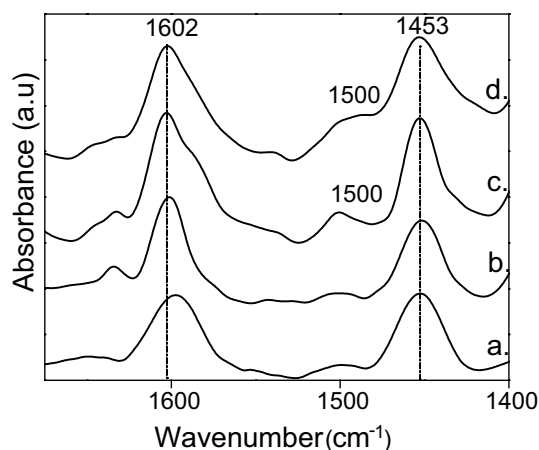
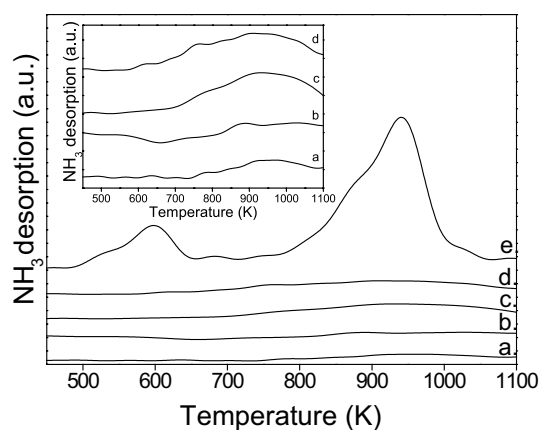
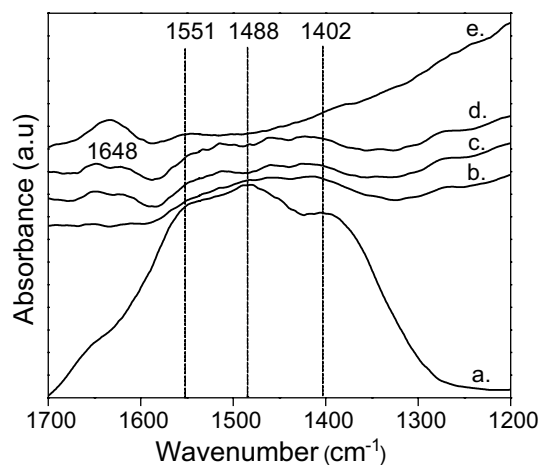
The X-ray diffraction patterns of Nb₂O₅, La₂O₃ and LaOCl/Nb are shown in Fig. 1. Figure 1a shows the typical X-ray diffraction patterns of crystalline niobium pentoxide pseudo-hexagonal structure called TT-Nb₂O₅ phase (Nb₂O₅, JCPDS 28-0317) [19]. However, the signals at 2θ = 28.9° and 36.9° reveal a slight change to orthorhombic phase caused by calcination at 773 K [9, 19, 20]. In mixed oxides (Fig. 1b–d), it can be seen that the incorporation and calcination of LaCl₃ species did not modify Nb₂O₅ structure; however, the type of lanthanum oxide species on Nb₂O₅ surface could not be determined by XRD. The signals of single La₂O₃ were characteristic of hexagonal phase (Fig. 2e) [4].

The FTIR spectra of pyridine adsorbed on the surface of Nb₂O₅ and LaOCl/Nb are shown in Fig. 2. The bands at 1453 and 1602 cm⁻¹ after purging with helium at 673 K are associated with Lewis acid sites on the surface of Nb₂O₅ [9, 19–22]. It is well known that for single Nb₂O₅ and supported Nb₂O₅, the number of Lewis acid

sites is higher than the number of Brønsted acid sites [22, 23]. The synthesized solids did not exhibit bands of

Table 1 La₂O₃ content determined by EDX and textural properties for catalysts studied

Catalyst	% La ₂ O ₃ deposited	S _{BET} (m ² /g)	Pore size (nm)	Pore volume (cm ³ /g)
Nb ₂ O ₅	–	4	6.6	0.006
1% LaOCl/Nb	1.0	3	12.7	0.005
3% LaOCl/Nb	2.5	3	12.2	0.005
5% LaOCl/Nb	4.2	3	12.5	0.005
La ₂ O ₃	–	5	11.6	0.00003

**Fig. 1** X-ray patterns of catalysts: (a) Nb₂O₅ single, (b) 1% LaOCl/Nb, (c) 3% LaOCl/Nb, (d) 5% LaOCl/Nb, (e) La₂O₃. Note peak assignments: *open square* pseudo-hexagonal phase of single Nb₂O₅, *open circle* orthorhombic phase of single Nb₂O₅, *open diamond* hexagonal phase of La₂O₃**Fig. 2** FTIR spectra of pyridine adsorbed at 423 K for (a) single Nb₂O₅, (b) 1% LaOCl/Nb, (c) 3% LaOCl/Nb, (d) 5% LaOCl/Nb**Fig. 3** Ammonia desorption patterns for (a) single Nb₂O₅, (b) 1% LaOCl/Nb, (c) 3% LaOCl/Nb, (d) 5% LaOCl/Nb, (e) single La₂O₃. The inset includes a–d only**Fig. 4** FTIR spectra of CO₂ adsorbed at 308 K for (a) single La₂O₃, (b) 1% LaOCl/Nb, (c) 3% LaOCl/Nb, (d) 5% LaOCl/Nb, (e) single Nb₂O₅

pyridine adsorption corresponding to Brønsted acid sites (1540 and 1655 cm⁻¹).

The temperature programmed desorption of ammonia (TPD-NH₃) profiles for the catalysts are shown in Fig. 3. The desorption of ammonia below 473 K is related to weak acid sites [24]; the range of 473–623 K corresponds to moderate strength acid sites, whereas at temperatures higher than 623 K it can be associated with strong acid sites [25]. Lanthanum oxide presented higher intensities of NH₃ desorption compared with niobium oxide and LaOCl/Nb mixed oxides. The intensity of NH₃ desorption for Nb₂O₅ and mixed oxides was quite similar, although, as observed in the inset, an increase in LaOCl content augmented the signal corresponding to strong acid sites. This can be associated with the generation of new

Lewis-type acid sites by the inclusion of LaOCl on the niobium oxide surface, providing higher acid strength.

The basicity of solids was studied by FTIR of CO₂ and TPD-CO₂. Figure 4 shows the spectra of CO₂ desorbed at room temperature on the surface of catalysts followed by FTIR. The region of 1700–1200 cm⁻¹ was chosen due to the possibility of differentiating bicarbonate and carbonate species. These two species are characteristic of stronger and labile basic sites, respectively [26].

A broad band in the spectral range 1700–1200 cm⁻¹ is observed on the surface of La₂O₃; the shoulders at 1402 and 1488 cm⁻¹ are attributed to symmetric stretching of unidentate carbonate species [27], while the band at 1551 cm⁻¹ is associated with asymmetric stretching due to the adsorption of CO₂ on basic sites of moderate strength [26, 27]. Furthermore, the synthesized solids also present a band located around 1648 cm⁻¹, which is attributed to bicarbonate species formed by interaction of CO₂ with the surface [27]. In the mixed oxides the contribution of carbonate and bicarbonate species increased with the content of LaOCl. The band at 1648 cm⁻¹ not was observed in the case of 1%/LaOCl/Nb catalyst. The lower absorbance intensities for the mixed oxides are directly related to La₂O₃ content. Besides, niobium oxide did not show any change in its spectrum after adsorption time, in agreement with that reported by Izuka et al. [24].

Temperature programmed desorption patterns of CO₂ (CO₂-TPD) for the catalysts are shown in Fig. 5. In the case of La₂O₃, the desorption of CO₂ at 473 K showed the existence of OH⁻ groups associated with weak basic sites [28], the signal around of 623 K corresponding to moderate strength basicity, which can be associated with bidentate carbonate species adsorbed on the catalyst surface [27].

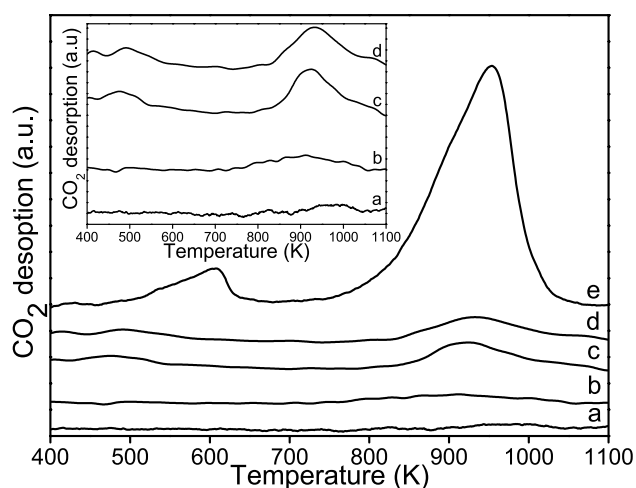


Fig. 5 CO₂ desorption patterns for (a) single Nb₂O₅, (b) 1% LaOCl/Nb₂O₅, (c) 3% LaOCl/Nb₂O₅, (d) 5% LaOCl/Nb₂O₅, (e) single La₂O₃. The inset includes a–d only

The desorption signal at 923 K is related to strong basic sites associated with unidentate carbonate species, as has been indicated in the literature [26, 29]. Desorption patterns for Nb₂O₅ and LaOCl/Nb₂O₅ are shown in the inset, where the formation of new weak and strong basic sites is clearly seen.

3.2 Catalytic Activity

3.2.1 Fructose Dehydration to HMF

Initially, the activity of Nb₂O₅, La₂O₃ and 3% LaOCl/Nb were tested in the production of HMF at 453 K using a 0.046 M solution of fructose in inert atmosphere. Table 2 shows the conversion and yields to HMF for each catalyst after 3 h of reaction. With the aim to assess whether fructose dehydration was promoted or not by the acidic properties of hot compressed water, the reaction was performed at different temperatures. The results are shown in Table 2. As can be observed, an increase in the reaction temperature increased the conversion and yield to HMF, this effect was more pronounced when the temperature reached 453 K, being possible that the fructose dehydration reaction was conducted alone by acidic properties of subcritical water state. However, when Nb₂O₅ was used as catalyst at 453 K the yield to HMF increased (85%), in the case of La₂O₃ HMF yield was 56%, and with 3% LaOCl/Nb catalyst HMF yield was 89%. Nb₂O₅ contains Lewis-type acid sites, while La₂O₃ has essentially basic sites. It can be observed that with La₂O₃ the interconversion to glucose occurs, however, the surface acid sites leads to a better catalytic performance in this reaction, thus niobia is the main active component

Table 2 Dehydration of fructose to HMF in a batch reactor after 3 h of reaction using different catalysts and temperatures

Conditions	α . (%)	Y (%) glucose	Y (%) HMF
393 K/without catalyst	2	1	1
413 K/without catalyst	11	4	7
423 K/without catalyst	23	1	22
453 K/without catalyst	87 ^a	1	34
453 K/Nb ₂ O ₅	94 ^a	1	85
453 K/La ₂ O ₃	97 ^a	8	56
453 K/3% LaOCl/Nb	97 ^a	2	89
333 K/3% LaOCl/Nb	2 ^a	0	0
353 K/3% LaOCl/Nb	5	5	0
373 K/3% LaOCl/Nb	7 ^a	0	1

Reaction conditions: 100 mg of the catalyst, a solution of fructose (0.046 M) using water as solvent

^aOthers products were not identified, thus the sum of reaction yields is not equal to conversion obtained

in dehydration of fructose in mixed oxides, similar finding were reported for $\text{CeO}_2\text{-Nb}_2\text{O}_5$ catalysts [22].

The results at lower temperatures were included in Tables 2 and 4. Thus, the catalytic evaluation was performed in a broad range of temperatures (333–473 K), evidencing that the formation of HMF from fructose or glucose is only reached at temperatures higher than 373 K. It has been reported [30] that the activation energy associated with undesirable side reactions is less (60 kJ/mol) than the related to the formation of HMF (140 kJ/mol) and consequently the HMF yield tends to increase with a higher temperature, but its value is influenced by the nature of the reaction system. Our results with $\text{LaOCl/Nb}_2\text{O}_5$ demonstrated that although the dehydration step of fructose could be stimulated by noncatalytic processes (conditions of hot compressed water at 273–647 K), the presence of catalysts avoids the side reactions. Thus, a synergic effect between the hot compressed water and the acid–base bifunctionality of $\text{LaOCl/Nb}_2\text{O}_5$ resulted in an increase in HMF yield. Another important fact is that when the reaction temperature is that when reaction temperature increased, water density increases, so that the yields towards HMF are clearly improved.

3.2.2 Glucose Dehydration to HMF

Table 3 shows the results of glucose dehydration at 3 h of reaction. When the reaction was conducted from glucose in the absence of catalyst values of conversion and yield were too low, as reported by Hu et al. [31, 32]. Therefore, although hot compressed water favors the production of HMF from fructose, but it does not favor HMF formation from glucose. The addition of the solids catalyst enhanced this reaction, however with single oxides presented higher glucose conversions but showed low yields to HMF. It has been demonstrated that this reaction requires a balance between acidic and basic sites [8,

31], a condition that is not fulfilled by La_2O_3 or Nb_2O_5 . In addition, it should be noted that in these reactions the mass balance is not reached, which is attributed to the formation of other compounds not identified in this study, as was described in experimental part. The use of acid–base systems for HMF production mainly from glucose requires weak basic sites and moderate acidity [33]. LaOCl/Nb mixed oxides present surface properties of both acid and basic sites as confirmed by acidity and basicity analyses. Although LaOCl/Nb mixed oxides presented lower conversion of glucose than La_2O_3 , they showed higher yields to HMF. 3% LaOCl/Nb showed the best yield to HMF (50%). The order of conversion and yield was 1% LaOCl/Nb < 5% LaOCl/Nb < 3% LaOCl/Nb . The inclusion of LaOCl on the surface of niobium oxide modified the ratio between acid and basic sites as compared to the single oxides, altering the yield to HMF and preventing the formation of other products. Consequently, in the case of mixed oxides, there are a higher number of strong basic sites than for single Nb_2O_5 . However, an excess of strong basic sites generates other compounds as in the case of single La_2O_3 . The dehydration of glucose to HMF in hot compressed water conditions requires strong basic sites with Lewis acid sites in order to obtain good yields to HMF. Besides, the possibility of a better dispersion of LaOCl species on Nb_2O_5 surface could explain the activity in 3%/ LaOCl/Nb .

Table 4 displayed the effect of reaction temperature on 3% LaOCl/Nb also was studied. The results showed that the conversion of glucose to HMF increased with reaction temperature as expected. However, the yield to HMF reached a maximum at 453 K, in agreement with the literature [34, 35]. Above this temperature, the yield to HMF decreases dramatically, which is attributed to the generation of secondary reactions forming products that are adsorbed on the catalyst surface [36], limiting the

Table 3 Catalytic results at 3 h using different catalysts in the dehydration of glucose

Conditions	Conv. (%)	Y (%) fructose	Y (%) HMF
Blank, without catalyst	22 ^a	1	14
Nb_2O_5	73 ^a	1	23
La_2O_3	92 ^a	2	23
1% LaOCl/Nb	48 ^a	3	43
3% LaOCl/Nb	58 ^a	6	49
5% LaOCl/Nb	54 ^a	5	45

Reaction conditions: 100 mg of the catalyst, a solution of glucose (0.046 M) using water as solvent at 453 K, and at 1000 rpm

^aOthers products were not identified, thus the sum of reaction yields is not equal to conversion obtained

Table 4 Catalytic results at 3 h using different reaction temperatures in the dehydration of glucose

Reaction temperature	Conv. (%)	Y (%) fructose	Y (%) HMF
333 K	1 ^a	0	0
353 K	2 ^a	0	0
373 K	3 ^a	0	0
413 K	14 ^a	8	5
433 K	34 ^a	9	21
453 K	58 ^a	6	49
473 K	88 ^a	2	24

Reaction conditions: 100 mg of the catalyst 3% LaOCl/Nb , a solution of glucose (0.046 M) using water as solvent at 1000 rpm

^aOthers products were not identified, thus the sum of reaction yields is not equal to conversion obtained

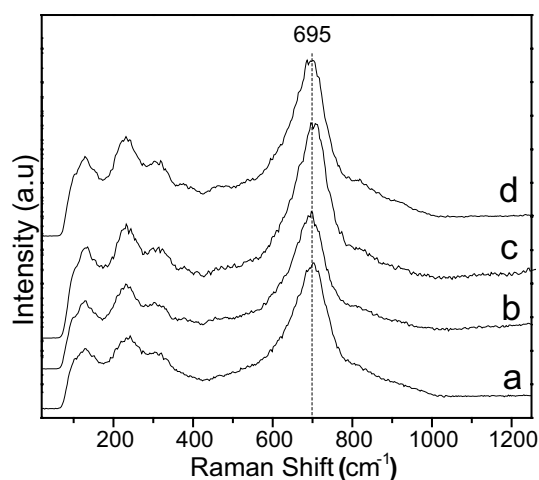


Fig. 6 Raman spectra submitted at hydrothermal treatment (a) single Nb₂O₅, (b) 1% LaOCl/Nb₂O₅, (c) 3% LaOCl/Nb₂O₅, (d) 5% LaOCl/Nb₂O₅

Table 5 Catalytic results at 3 h using 3% LaOCl/Nb calcined to distinct temperatures

Conditions	Conv. (%)	Y (%) fructose	Y (%) HMF
LaCl ₃ used without calcination	59 ^a	3	35
3% LaOCl/Nb calcined at 573 K	53 ^a	1	26
3% LaOCl/Nb calcined at 673 K	61 ^a	1	30
3% LaOCl/Nb calcined at 773 K	58 ^a	6	49

Reaction conditions: 100 mg of the catalyst, 453 K, a solution of glucose (0.046 M) using water as solvent and at 1000 rpm

^aOthers products were not identified, thus the sum of reaction yields is not equal to conversion obtained

transformation of glucose into HMF. The formation of undesirable compounds is clearly seen in the coloration showed by the catalyst after being filtered; this coloration is typical of the presence of humins [37].

The calcined and dried Nb₂O₅ and Nb₂O₅/La₂O₃ oxides present only Lewis acid sites, as confirmed by FTIR-Py. However, to clarify the effect of hydrothermal treatment on the sample acidity, we studied the solids by Raman spectroscopy after a hydrothermal treatment at 453 K for 2 h. The Raman spectra of LaOCl/Nb₂O₅ submitted to hydrothermal treatment are shown in the Fig. 6. A major niobium oxide Raman band at 550–750 cm⁻¹, assigned to NbO₆ octahedra. This band is not modified by the content of LaOCl. Another interesting fact is the absence of the band at 988 cm⁻¹ that is attributable to NbO₄ tetrahedra. The absence of this band indicates a possible formation of NbO₄–H₂O adducts [38]. The NbO₄–H₂O adducts are related to Lewis acidity [38–40], so there was not any change in the type of acid site under the reaction conditions.

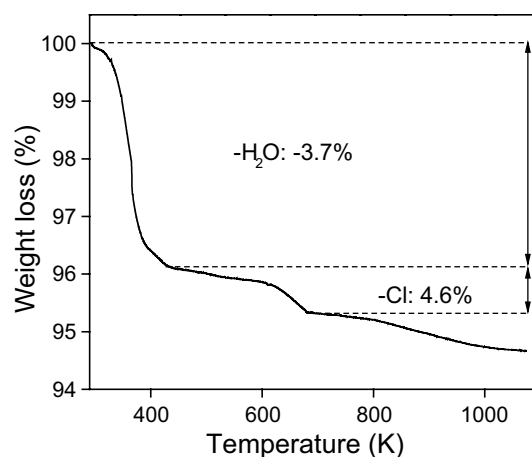


Fig. 7 Thermogram of LaOCl/Nb₂O₅ catalyst

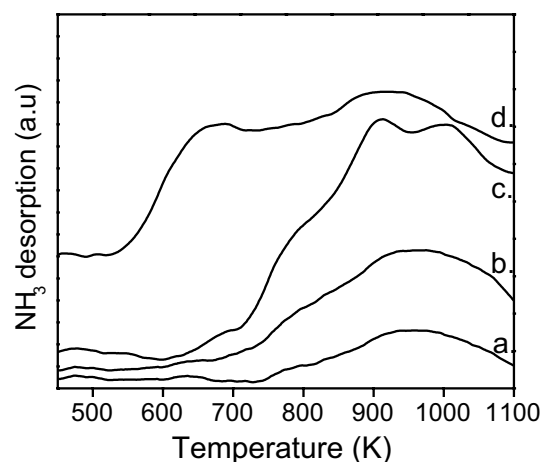


Fig. 8 Ammonia desorption patterns for (a) single Nb₂O₅, (b) 3% LaOCl/Nb calcined at 773 K, (c) 3% LaOCl/Nb calcined at 673 K, (d) 3% LaOCl/Nb calcined at 573 K

To understand the interaction of LaOCl on Nb₂O₅ the effect of temperature of calcination was studied. The solid impregnated 3%/LaOCl/Nb was submitted to calcination at 573, 673 and 773 K. It can be seen in the Table 5 that LaOCl/Nb presented a higher yield to HMF only after calcination at 773 K. After calcination at 573 and 673 K LaOCl/Nb behavior was similar to LaCl₃ which was used in the synthesis of solids. The TGA profile of 3% LaOCl/Nb₂O₅ (Fig. 7) revealed that only at 640 K a new phase was formed which could be responsible for catalytic activity. The two weight losses in TGA profile (at 420 and 640 K) are due to the removal of water (on the surface or structural) and possibly to liberation of chloride residues, respectively. The new phase formed at 643 K is due to calcination of LaCl₃ to LaOCl. Thus, calcination at 773 K assured a conversion of LaCl₃ to LaOCl and prevented the formation of La₂O₃ [17].

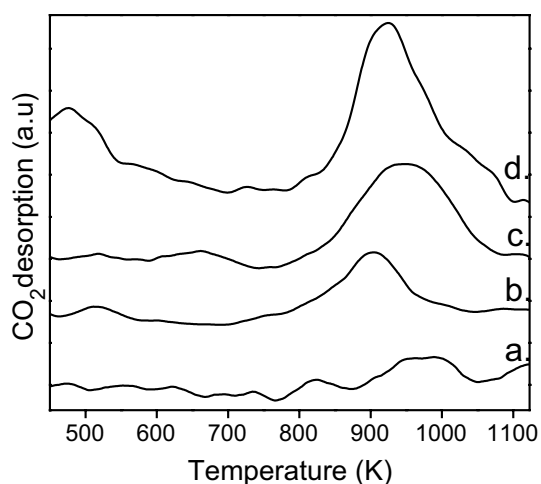


Fig. 9 CO₂ desorption patterns for (a) single Nb₂O₅, (b) 3% LaOCl/Nb calcinated at 573 K, (c) 3% LaOCl/Nb calcinated at 673 K, (d) 3% LaOCl/Nb calcinated at 773 K

A comparison between the Lewis acidity of different lanthanum phases with probe molecules showed a general trend in which surface acidity increases, and conversely, surface basicity decreases in the following order: La₂O₃ > LaOCl > LaCl₃ [28]. This behavior is clearly observed in the NH₃-TPD and CO₂-TPD of solid impregnated 3% LaOCl/Nb submitted to calcination at 573, 673 and 773 K (Figs. 8, 9). The NH₃-TPD of LaOCl/Nb at 473 K showed two signals at around 650 K and another at 950 K, when the solid is calcined at 673 or 773 K, the signal at 650 K disappears. In the same manner, in the CO₂-TPD of LaOCl/Nb at 473 K showed two signals around at 450 and 950 K, the first signal disappearing at 673 K. Possibly, the signals that disappear with an increase in the calcination temperature are characteristic of LaCl₃ species. This behavior is well related to TGA results, showing that the calcination at 773 K assured a conversion of LaCl₃ to LaOCl and prevented the formation of La₂O₃ [17].

A correlation between the acidity of different lanthanum phases in the dehydration of glucose (Table 5) showed that a higher acidity does not assure a higher yield to HMF. In fact, the yield of HMF using LaCl₃ is only 35% (Table 5), while with La₂O₃ is 23% (Table 3). Thus, the moderate acidity of 3% LaOCl is necessary for catalyzing the dehydration of fructose to HMF. When the amount of LaOCl is 5% the yield to HMF also decreases (45%). The deposition of LaOCl improves the acidity of Nb₂O₅ and promotes the isomerization of glucose to fructose, favoring the conversion and the yield to HMF. Besides, the use of LaOCl/Nb₂O₅ shows a high stability, as was demonstrated by the Raman Spectra.

Figure 10 shows a typical conversion/yield versus time graph for 3% LaOCl/Nb. The presence of HMF is

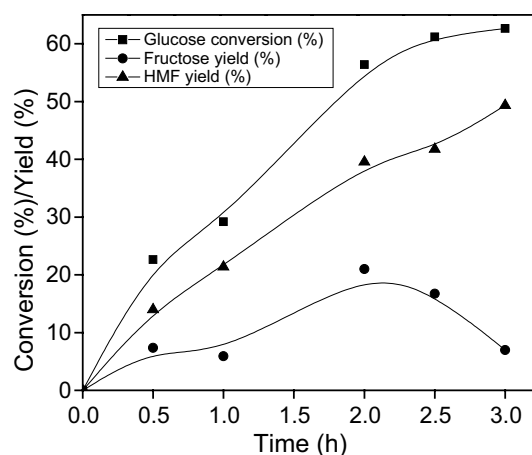


Fig. 10 Conversion/yield versus time of reaction for 3% LaOCl/Nb at 453 K

evidenced at 1 h of reaction, which demonstrates that the formation of fructose as a reaction intermediate is necessary, being the rate determining reaction [39, 41]. Besides, it can be seen that a maximum yield to fructose is reached at 2 h of reaction, which is then transformed into HMF. However the final solution presented a dark color, which can be associated with humins formation [37].

In the Fig. 10 is shown that the conversion of LaOCl/Nb₂O₅ increases with the reaction time and reaches a plateau at the time of 3 h (data not shown), the maximum yield to fructose is reached at 2 h of reaction. Short reaction time (30 min) gives 75% selectivity but low substrate conversion (22%). However, an increase in the reaction time led to an increase in conversion but lower selectivity to HMF. Long times contribute to the formation of by-products due to decomposition of HMF in humins, levulinic acid, formic acid, and other condensation products. However, the transformation of HMF, deriving from the dehydration of fructose or glucose, into LA markedly depends on the nature and concentration of the acid used as catalyst. The main advantage of the use of Nb₂O₅ as catalysts is the absence of side reactions in the dehydration reaction of fructose to HMF in water; although, the deposition of LaOCl improves the acidity of Nb₂O₅ and promotes the isomerization of glucose to fructose, favoring the conversion and the yield to HMF, it depends of LaOCl content and temperature used in the reaction.

The results obtained for the prepared catalysts are compatible with values reported for reactions of dehydration of fructose and glucose in organic media at similar reaction temperatures [4, 7, 10, 29, 38, 42]. Hence, the significance of these results are due to the fact that the reactions were carried out in conditions of hot compressed water, without the use of organic solvents. In order to further investigate the effect of solvent, the reactions in DMSO, DMSO/H₂O

Table 6 Catalytic results of dehydration of glucose using different solvents

Solvent	Conv. (%)	Y (%) fructose	Y (%) HMF
H ₂ O	58 ^a	6	49
1/1 H ₂ O/DMSO	48 ^a	13	39
DMSO	65 ^a	8	53

Reaction conditions: 100 mg of the catalyst 3% LaOCl/Nb, a solution of glucose (0.046 M), at 1000 rpm, at 3 h of reaction

^aOthers products were not identified, thus the sum of reaction yields is not equal to conversion obtained

Table 7 Catalyst recycles of 3% LaOCl/Nb

Cycles	Conv. (%)	Y (%) fructose	Y (%) HMF
1	58 ^a	6	49
2	52	2	50
3	49 ^a	4	39
4	39 ^a	3	35

Reaction conditions: 100 mg of the catalyst, a solution of glucose (0.046 M) using water as solvent, at 1000 rpm, at 3 h of reaction

^aOthers products were not identified, thus the sum of reaction yields is not equal to conversion obtained

(1/1) and H₂O were investigated. It can be seen in Table 6 that when the reaction was conducted in DMSO, yield to HMF (53%) was slightly highest than when hot water was used as solvent (49%). In the presence of DMSO there is preferential coordination between fructose and HMF molecules preventing side reactions [43]. A mixture of DMSO/H₂O used as solvent decreased both the conversion and yield, indicating that the solvent influences the rate determining step [44], i.e., the formation of fructose affects the HMF yield.

Finally, the reuse of catalysts was studied in four cycles of reaction (Table 7). As a result of the second cycle of reuse, the catalyst yield slightly increased toward HMF (52%), but the results for the other cycles showed a clear decrease in the yield toward HMF, possibly, this is related to the change of acid and basic sites present on the catalyst surface, due to the formation of soluble polymers and humins that favors the deactivation of the catalyst [35, 37, 45, 46].

4 Conclusions

The deposition of LaOCl species on Nb₂O₅ generates new acidic and basic sites, providing Lewis acid sites and strength basic sites. These solids were active for the production of HMF from glucose and fructose in conditions of hot compressed water (453 K). 3% LaOCl/Nb₂O₅ calcinated at

773 K after 3 h of reaction reaching a maximum 89 and 49% yield HMF from fructose and glucose, respectively. A synergetic effect between the hot compressed water and the Lewis acidity sites of NbO₄-H₂O adducts favored the HMF formation from fructose.

Acknowledgements We thank COLCIENCIAS for the financial support under Project No. 110965843004. FBP and MHB thank FAPERJ and CNPq for financial support.

References

- Rosatella AA, Simeonov SP, Frade RFM, Afonso CAM (2011) *Green Chem* 13:754
- Yang G, Pidko EA, Hensen EJM (2012) *J Catal* 295:122–132
- Wang J, Xu W, Ren J, Liu G, Wang Y (2011) *Green Chem* 13:2678
- Yang F, Liu Q, Yue M, Bai X, Du Y (2011) *Chem Commun* 47:4469–4471
- Tao F, Zhuang C, Cui Y, Xu J (2014) *Chin Chem Lett* 25:757–761
- Yan H, Yang Y, Tong D, Xiang X, Hu C (2009) *Catal Commun* 10:1558–1563
- Dunn EF, Liu DDJ, Chen EY (2013) *Appl Catal A* 460–461:1–7
- Siqueira BG, Silva MAP, Moraes C (2013) *Braz J Pet Gas* 7:71–82
- Wang F, Wu HZ, Liu CL, Yang RZ, Dong WS (2013) *Carbohydr Res* 368:78–83
- Yang F, Liu Q, Bai X, Du Y (2011) *Bioresour Technol* 102:3424–3429
- Carniti P, Gervasini A, Biella S, Auroux A (2006) *Catal Today* 118:373–378
- Yue C, Li G, Pidko EA, Wiesfeld JJ, Rigutto M, Hensen EJM (2016) *ChemSusChem* 17:2421–2429
- Jiao H, Zhao X, Lv C, Wang Y, Yang D, Li Z, Yao X (2016) *Sci Rep* 6:1–9
- Huang Z, Pan W, Zhou H, Qin F, Xu H, Shen W (2013) *ChemSusChem* 6:1063–1069
- Watanabe M, Aizawa Y, Iida T, Aida TM, Levy C, Sue K, Inomata H (2005) *Carbohydr Res* 340:1925–1930
- Nayara T, Souza TE, Rodrigues A, Machado T, Souza PP, Monteiro RS (2016) *J Mol Catal A* 422:23–34
- Marsal A, Rossinyol E, Bimbela F, Téllez C, Coronas J, Cornet A, Morante JR (2005) *Sens Actuators B* 109:38–40
- Rojas HA, Borda G, Valencia JS, Martínez JJ, Reyes P (2005) *Rev Colomb Quím* 34:127–138
- Murayama T, Chen J, Hirata J, Matsumoto K, Ueda W (2014) *Catal Sci Technol* 4:4250–4257
- Kitano T, Shishido T, Teramura K, Tanaka T (2012) *J Phys Chem C* 116:11615–11625
- Ohuchi T, Miyatake T, Hitomi Y, Tanaka T (2007) *Catal Today* 120:233–239
- Bennici S, Raki V (2012) *Catal Today* 192:160–168
- Datka J, Turek AM, Jehng JM, Wachs IE (1992) *J Catal* 135:186–199
- Iizuka T, Ogasawara K, Tanabe K (1983) *Bull Chem Soc Jpn* 56:2927–2931
- Rangel MDC, Monteiro APDM, Marchetti SG et al (2014) *J Mol Catal A* 387:147–155
- Liu Q, Wang L, Wang C, Qu W, Tian Z, Ma H, Wang D, Wang B, Xu Z (2013) *Appl Catal B* 136–137:210–217
- Shen SC, Chen X, Kawi S (2004) *Langmuir* 20:9130–9137

28. Manoilova OV, Podkolzin SG, Tope B, Lercher J, Stangland EE, Goupil J, Weckhuysen BM (2004) *J Chem Phys B* 108:15770–15781
29. Zhang J, He D (2014) *J Colloid Interface Sci* 419:31–38
30. Do Prado NT, Souza TE, Machado ART, Souza PP, Monteiro RS, Oliveira LCA (2016) *J Mol Catal A* 422:23–34
31. Hu L, Wu Z, Xu J, Sun Y, Lin L, Liu S (2014) *Chem Eng J* 244:137–144
32. Hu L, Sun Y, Lin L (2012) *Ind Eng Chem Res* 51:1099–1104
33. Ohara M, Takagaki A, Nishimura S, Ebitani K (2010) *Appl Catal A* 383:149–155
34. Zhang Y, Wang J, Li X, Liu X, Xia Y, Hu B, Lu G, Wang Y (2015) *Fuel* 139:301–307
35. Jiménez-Morales I, Santamaría-González J, Jiménez-López A, Maireles-Torres P (2014) *Fuel* 118:265–271
36. Jiménez-Morales I, Moreno-Recio M, Santamaría-González J, Maireles-Torres P, Jimenez-López A (2014) *Appl Catal B* 154–155:190–196
37. Rasmussen H, Sørensen HR, Meyer AS (2014) *Carbohydr Res* 385:45–57
38. Nakajima K, Baba Y, Noma R, Kitano M, Kondo J, Hayashi S, Hara M (2011) *J Am Chem Soc* 133:4224
39. Jehng J-M, Wachs IE (1991) *Chem Mater* 3:100–107
40. Hara M (2014) *Bull Chem Soc Jpn* 87:931–941
41. Wachs IE, Roberts CA (2010) *Chem Soc Rev* 39:5002–5017
42. Van Putten R, Van Der Waal JC, De Jong E et al (2013) *Chem Rev* 113:1499–1597
43. Qi X, Watanabe M, Aida TM, Smith RL (2010) *Green Chem* 12:1855–1860
44. Shimizu K, Uozumi R, Satsuma A (2009) *Catal Commun* 10:1849–1853
45. Jain A, Shore AM, Jonnalagadda SC, Ramanujachary KV, Mugweru A (2015) *Appl Catal A* 489:72–76
46. Alam MI, De S, Singh B, Saha B, Abu-Omar MM (2014) *Appl Catal A* 486:42–48